Compressive Strength of Foamed Polymeric Piling

Presentated at

TRB 2003 SESSION ON FIBER REINFORCED POLYMER PILES

(SPONSORED BY COMMITTEES A2K03 & A2K01)

(Paper No: 03-2448)

by

Magued Iskander, PhD, PE,
Associate Professor, Polytechnic University
6 Metrotech Center, Brooklyn, NY 11201
Phone: (718) 260-3016
Fax: (718) 260-3433
Email: Iskander@poly.edu

Ahmed Mohamed
Geotechnical Engineer, GZA Geoenvironmental of New York
2 Penn Plaza, New York, NY 10121
Phone: (212)594-8140
Fax: (212)279-8180
Email: Amohamed@gza.com

Samer Sadek, PhD
Tunnel Engineer, Parsons Brinkerhoff Quade & Douglas, Inc.
One Penn Plaza, New York, NY 10119
Phone (212) 643-4747
Fax: (212) 695-8762
Email: Ssadek@mta-esa.org

Compressive Strength of Foamed Polymeric Piling

Magued G. Iskander, PhD, PE, Ahmed Mohamed, and Samer Sadek, PhD

Magued Iskander, PhD, PE, Associate Professor, Polytechnic University, 6 Metrotech Center, Brooklyn, NY 11201
Ahmed Mohamed, Geotechnical Engineer, GZA Geoenvironmental of New York, New York, NY 10121
Samer Sadek, PhD, Tunnel Engineer, Parsons Brinkerhoff Quade & Douglas, Inc., One Penn Plaza, NY, NY 10119

Abstract. Fiber reinforced polymer (FRP) composites represent an alternative construction material without many of the performance disadvantages of traditional materials. The use of FRP as a pile material can eliminate deterioration problems of conventional piling materials in water front environments and aggressive soils. A comprehensive understanding of the mechanical properties of foamed polymers is essential for widespread use of polymeric piling.

This paper presents the results of an experimental study conducted to assess the spatial distribution of the compressive strength of piling made of foamed recycled plastics. The strength and unit weight increased exponentially with distance from the center. Strength was found linearly proportional to the unit weight of the piling specimens, and inversely proportional to the degree of foaming. Dimensional and regression analyses were used to reduce data scatter and define the spatial distribution of strength. Finally, a procedure for obtaining the stress strain curve of the full scale foamed polymeric piling based on testing of small coupon specimens was presented.

INTRODUCTION

There has been increasing interest in the use of fiber reinforced polymeric (FRP) composite materials in piling (1). This trend is expected to grow since polymeric piling represents a creative solution for two long-standing problems. The first is that deterioration of timber, concrete, and steel piling systems costs the United States nearly $1 billion per year for repair and replacement (2). The second is that in the United States over 7.2 billion pounds of rigid plastic containers are annually buried in landfills (3). Most of these containers are made of high-density polyethylene (HDPE) milk jugs, and polyethylene-terephalate (PET) soda bottles.

In the case of marine piling, actions required by the federal Water Pollution Control Act of 1972 gradually rejuvenated many of the nation's waterways and harbors. A side effect of this environmental benefit is the return of marine borers, which started to attack the untreated timber piles that support many of the nation's harbor piers (4). Polymeric piling is a well suited replacement for timber piling.

Polymeric piling products are typically made of HDPE with fiberglass reinforcement and additives to improve their mechanical properties, durability, and ultraviolet (UV) protection. Polymer based resins are heavier than wood and foaming of the resin is often used to make the product lighter. The composite resin formulation is a complex process that involves optimizing cost and material properties in order to achieve the desired performance. The manufacturing process and the use of recycled materials results in products that are often heterogeneous and anisotropic.

Plastic lumber, like polymeric piling, is also produced using a complex manufacturing process that involves foaming of the lumber. Therefore, ASTM standards dealing with plastic lumber call for testing the full structural member, instead of small coupon specimens, which is popular for conventional construction materials. At the present time, standards for testing of FRP piling are being developed and will involve testing of the full cross section. A better understanding of the spatial distribution of the compressive properties may lead to use of coupon specimens for quality control of polymeric piling and plastic lumber.

This paper presents the results of an experimental study conducted to characterize the compressive strength of foamed polymeric piling. ASTM D695-96 Standard Test Method for Compressive Properties of Rigid Plastics was used to define the spatial distribution of strength.

AVAILABLE FOAMED POLYMERIC PILING

In Summer 2002, there are two types of foamed polymeric products that are available for use in piling, as follows:

Reinforced Plastic Piling

These piles typically consist of an extruded recycled High Density Polyethylene (HDPE) plastic matrix reinforced with fiberglass or steel rods (Fig. 1). Additives are used to improve mechanical properties, durability, and ultraviolet (UV) protection. A foaming agent is used to make the product lighter. The matrix may also contain a small percentage of fiberglass to enhance its physical properties. Seaward International, Inc. and Plastic Piling Inc., produce piles of this type. Piles are available in 25–40 cm (10–16 in.) diameters and are reinforced with 6–16 reinforcing bars ranging in diameter between 25 and 36 mm (1–1.41 in). Reinforced plastic piling has existed for approximately 10 years. So far, it has been used primarily to resist lateral ship impact (fendering).

Plastic Lumber

Fiber reinforced plastic piling consists of a recycled plastic matrix with randomly distributed fiberglass reinforcement in the matrix. A foaming agent is used to make the product lighter. Additives are also used to improve mechanical properties, durability, and ultraviolet (UV) protection. US Plastics and American Echo Board manufacture this product. The manufacturers produce a variety of structural members that conform to lumber industry standards. Piling is available in 25–40 cm (10–16 in.) diameter with in a standard length of 6–7.5 m (18–24 ft.), but longer lengths could be custom made. In the last decade, plastic lumber has established a good track record in residential construction. However, use of the product in piling has been limited to demonstration and experimental projects.

TESTING PROGRAM

Test Specimens

Seapile™ which is a reinforced plastic piling product made by Seaward International, Inc. (5) was used (Fig. 1). Seapile™ is produced in two stages. First, a core made of foamed recycled

HDPE is produced. Next, structural reinforcement is added and additional recycled HDPE is molded around the core. Seaward mixes proprietary additives and fiberglass reinforcement with the HDPE to enhance the properties of the pile matrix.

Seaward provided us with saw cut cross-sections, 20 cm in diameter and 2–5 cm thick, which are referred to hereinafter as *wafers*. These wafers were taken from the core of the pile's cross-section. All wafers came from adjacent locations in the same pile. First, wafers were machined to ensure that both surfaces were parallel. Next, cylindrical specimens having a length to diameter ratio of 2: 1 were punched out of these wafers (Fig. 1) using thin metal cylindrical-cutters. The specimens were color coded in order to keep track of the locations where they were extracted. The weights, lengths, volumes, and densities of all specimens tested in this program were recorded.

Compression Tests

Compression testing was selected to characterize the spatial distribution of strength because piles are typically subjected mainly to compression loading. Specimens were tested in unconfined compression according to ASTM D695 (6). A computerized loading frame permitting displacement controlled compression testing was used. The specimens were tested at a strain rate of 15%/min. to a strain of 25%. Load and deformation were measured electronically.

For rigid plastics, the standard test specimen for ASTM D695 is a right cylinder or a prism whose length is twice its principal width or diameter. The preferred specimen size for a cylindrical specimen is 12.7 mm in diameter by 25.4 mm length.

Testing matrix

A total of 75 specimens were tested. Specimens having four diameters of 6.4, 9.5 12.7, 19 mm (1/4, 3/8, 1/2, 3/4 in) were tested in order to study the effect of the specimen size on the measured compressive strength. All specimens had a length to diameter ratio of 2:1.

One wafer was used to extract specimens for each of the specimen diameter tested. The center of each wafer was defined as its origin (Fig. 2). Specimens were extracted from several rows within each wafer, such that specimens corresponding to each row are all extracted from an equal distance from the origin. This was done to study the spatial distribution of compressive strength within the pile's cross section.

Polymeric materials typically exhibit a large variation in strength. Therefore, five specimens were tested from each row-diameter combination, as required by ASTM D695.

TEST RESULTS

The stress strain curves for all tested specimens are shown in Fig. 3–6. Individual tests are shown using thin solid lines, and the heavy dashed line represents the numerical averages of the data. The average lines are plotted again in the lower right corner of each figure to facilitate comparison of the test results.

Specimens did not exhibit a defined failure point. Neither a yield strength nor a peak strength could be defined.

Spatial Distribution of Strength

The compressive strength of the tested specimens exhibits a significant scatter. Nevertheless, this scatter can be attributed to the spatial distribution of strength within the specimens. When eight stress strain curves are grouped according to the distance from the origin, as shown in Fig. 3–6, very little scatter is evident, and the average of these curves is indistinguishable from the original curves. Small variations from the average can be attributed to the use of recycled materials to manufacture Seapile™.

Variation in strength with distance from the origin can be attributed to several mechanisms that take place during the manufacture of foamed polymers, as follows:

- Seapile™, like many polymeric structural members, is foamed at the center and solid at the edges. This causes difference in densities across the cross section, with the center being less dense than the outer sections.
- The manufacturing process could have resulted in variation in strength of the parent material across the cross section, due to cooling of the outer sections faster than the internal ones.

Variation in strength with distance from the origin can be fitted using either a polynomial or an exponential function (Fig. 7); which is useful in describing the spatial properties of foamed polymers and reducing the need for full scale testing, as shown later in this paper.

Effect of Specimen Size

Due to the difference in the specimens' diameters, it was not possible to use the same radii for extracting specimens from different wafers. The strength measured using different specimen sizes was plotted against the distance from the origin at four representative strains in order to facilitate direct comparison of the results (Fig. 8).

A small specimen size effect can be seen, particularly at higher strains. Specimens with 9.5 mm and 12.5 mm (3/8 and 1/2") diameter exhibited a somewhat smaller strength than 6.4 and 19.1 mm (1/4 and 3/4") diameter specimens. This could have possibly resulted from a combination of the following factors:

- The imperfection sensitivity of foamed recycled polymers is probably influenced by the presence of inclusions such as air bubbles, reinforcing fibers, and material imperfections caused by the use of recycled plastics. These inclusions have mean sizes which can influence the formation of kink bands and the propagation of failure.
- Strength is expected to increase with decreasing specimen size if the initiation of failure is dependent on occurrence of a critical defect of a fixed size. The probability of having a critical crack is smaller in a smaller specimen, which causes the strength to be higher for the smallest specimens.
- As the specimen size increases, failure transitions from a macro-buckling mode to a micro-buckling or other strength dependant mechanism, which causes the largest specimens to have a higher strength.

- Residual stresses from punching or stress concentration at the perimeter of the specimen can influence the mechanism of failure

In any case, additional research is needed to verify the presence or lack of a size effect, particularly considering the widely reported variation in the strength of polymeric materials. Therefore, all specimen sizes are used in this paper to draw conclusions.

Spatial Distribution of Density

The density distribution of the tested specimens shown in Fig. 9 is remarkably similar to the distribution of strength within the specimens (Fig. 7, 8). Like strength, variation in density with distance from the origin can be fitted using either a polynomial or an exponential function

The relationship between density and strength is linear (Fig. 10), indicating that strength is linearly proportional to the mass of resin used to form the specimens and inversely proportional to the degree of foaming used in manufacturing.

REGRESSION ANALYSIS OF TEST RESULTS

A better understanding of the spatial distribution of compressive properties may lead to use of coupon specimens for quality control of polymeric piling and plastic lumber. To achieve this, an exponential model was used to curve fit the experimental test results shown in Fig. 7, as follows:

$$\sigma = m_0 \, e^{m_1 R} \tag{1}$$

where σ is the measured stress, R is radius, and m_0 and m_1 are constants. The term m_0 represents the material strength at the origin or center of the wafer (weakest point). Theoretically, it can be related to the materials initial secant modulus, E, and strain, ε, as follows:

$$m_0 = \sigma = E\varepsilon \tag{2}$$

m_1 is a constant that describes the spatial distribution of the strength in the cross section Both m_0 and m_1 depend on the strain (Table 1). m_1 was relatively stable and was approximately 0.18 for small strains (1-2%) and decreased to 0.15 for larger strains (5-10%). The value of m_0 was strongly influenced by the non-linearity of the secant modulus of polymers, and it was not possible to relate m_0 directly to the applied strain.

A better definition of the values of m_0 and m_1 is needed. Nevertheless, the utility of the exponential model of the spatial distribution of strength is illustrated next.

The total load carried by the foamed cross section can be calculated by integrating the stress, as follows:

$$Total\ \ Load = \int_0^{R_{max}} m_o e^{m_1 R}\ \ 2\pi R\ \ dR \tag{3}$$

$$Total\ \ Load = 2\pi \frac{m_0}{m_1}\left(R_{max} e^{m_1 R_{max}} - \frac{e^{m_1 R_{max}}}{m_1} + \frac{1}{m_1} \right) \tag{4}$$

The average stress, $\sigma_{average}$, can be obtained by dividing the total load by the cross sectional area, as follows:

$$\sigma_{average} = \frac{2m_0}{m_1 R_{\max}^{\ 2}}\left(R_{\max} e^{m_1 R_{\max}} - \frac{e^{m_1 R_{\max}}}{m_1} + \frac{1}{m_1} \right) \tag{5}$$

A stress strain curve for the full cross section can be predicted from testing done on coupon specimens by substituting in Eq. 5 using the values m_0 and m_1 shown in Table 1. The predicted stress strain curve is shown in Fig. 11 as the heavy black line. The thin lines are the average stress strain curves measured for the 9.5-mm (3/8") diameter specimens.

DIMENSIONAL ANALYSIS OF TEST RESULTS

Langhaar (7) defined dimensional analysis as "a method by which we deduce information about a phenomenon from the single premise that the phenomena can be described by a dimensionally correct equation among certain variables." As the number of variables affecting the problem increases, it becomes progressively more difficult to determine the function which relates the various variables involved. Buckingham π theorem is used to overcome this difficulty by grouping dependent and independent variables into a smaller number of non-dimensional products (8). These non-dimensional products are referred to as π terms.

The relevant parameters affecting the spatial distribution of stress, σ, are assumed to be the density of the individual specimens γ, and the radial distance from center of the wafer to the center of the specimen R. In order to obtain a non-dimension π term, the relevant parameters are arranged as follows:

$$(\gamma)^a (R)^b (\sigma)^c = 1 \tag{6}$$

where a, b, & c are any powers. The objective of this exercise is to define the values of a, b, and c. Expressing the terms by their fundamental dimensional units:

$$\left(\frac{F}{L^3}\right)^a (L)^b \left(\frac{F}{L^2}\right)^c = 1 \tag{7}$$

The following relationships can be obtained by equating the force and length powers:

$$a = -c \tag{8}$$

$$b = 3a + 2c$$

If $a = -1$, then $c = 1$ and $b = -1$

Substitute (3) in (1) yields

$$(\gamma)^{-1}(R)^{-1}(\sigma)^{1} = 1 \tag{9}$$

Thus, the relevant π term is:

$$\pi = \frac{\sigma}{\gamma \cdot R} \tag{10}$$

The non-dimensional term $\pi=\sigma/\gamma R$ is referred to as the *Characteristic Stress*, and is believed to be a unique signature property of foamed structural members. It can be understood in the context of a second-degree polynomial fit of the material, since unit weight can be assumed a linear function of the radius, R (Fig. 10).

The characteristic stress was used to reduce scatter for specimens taken from adjacent rows near the border (7, 10). For example, when the stress vs. strain of the specimens shown in Fig. 12a was first plotted, a large scatter was observed, even though the specimens were extracted from a 5 cm wide ring at the perimeter. When the characteristic stress is plotted against strain, the scatter essentially disappears as shown in Fig. 12b.

The average stress strain curves of all specimens tested (shown in the lower right corner of Fig. 3–6) are plotted again in Fig. 13. The characteristic stress was calculated, using Eq. 10. for the stress strain tests shown in Fig. 13 and is plotted in Fig. 14a. Eleven of the sixteen stress strain curves converged. The remaining 5 were for specimens located close to the center (R smaller or equal to 3.2 cm). The Characteristic stress, π, is useful in reducing scatter of specimens located near the edges but does not represent specimen behavior near the center of the pile. This may not necessarily be detrimental since most of the specimen strength is derived from the outer portion, which is stronger and represents 85% of the specimen cross sectional area.

Numerically the value of π approaches infinity as R approaches zero. π does a poor job of fitting the strength near the center because the strength of the specimens at the center is a smaller multiple of that at the edges, and is not infinitely smaller than that at the edges. The *Modified Characteristic Stress*, π_m is an attempt to capture this phenomenon. It is obtained simply by adding a constant *K* to the radius term, R, as follows

$$\pi_m = \frac{\sigma}{\gamma(R + K)} \tag{11}$$

The modified characteristic stress, π_m, of the stress strain tests shown in Fig. 14 is plotted in Fig. 15b. An arbitrary value of K =12 was used in Fig 14b. π_m is superior to π in reducing

overall data scatter. Nevertheless, it performed better for specimens located near the center than away from it, which is undesirable. In any case, both π and π_m are better suited for reducing the scatter of specimens taken from adjacent locations.

CONCLUSIONS

The compressive strength of the tested specimens exhibits a significant scatter and no specimens exhibited a defined failure point. Nevertheless, this scatter can be attributed to the spatial distribution of strength and density within the specimens. The strength and density of foamed polymeric piling increased exponentially with distance from the center of the pile. Strength was found linearly proportional to density and inversely proportional to the local unit weight.

An exponential model was presented to describe the spatial variation of strength within the cross section of foamed polymeric piling. The model was used to derive the stress strain curve for the full cross section using testing done on coupon specimens.

Dimensional analysis of the test results was also used to reduce data scatter, and obtain a singular stress strain curve. The dimensionless term $\pi=\sigma/\gamma R$ was found representative of the stress strain curves for all specimen located in the outer segment of the sample (R>3.5 cm).

ACKNOWLEDGMENTS

We thank the Federal Highway Administration, The Empire State Development Corporation, and the New York State Department of Economic Development for sponsorship of this work.

REFERENCES

1. Iskander, M and Hassan, M. (1998) "State of The Practice Review FRP Composite Piling," *ASCE Journal of Composites for Construction*, August, Vol.2, No. 3, pp. 116–120

2. Lampo, R., Nosker, T., Barno, D., Busel, J., Maher, A., Dutta, P., and Odello, R. (1998). *Development and Demonstration of FRP Composite Fender, Load-bearing, and Sheet Piling Systems,* Report, US Army Corps of Engineers, Construction Engineering Research Laboratories, Champaign, IL 61826-9005.

3. Lampo, R. (1995). "Recycled Plastics as an Engineered Material." *Proc. XIII Struct. Congress, Restructuring America and Beyond*, Sanayei, M., *ed.*, Vol. 1, pp. 815-818, ASCE, Reston, VA

4. Iskander, M and Stachula, A. (1999) "FRP Composite Polymer Piling An Alternative to Timber Piling For Water-Front Applications," *Geotechnical News*, vol. 17, No. 4, pp. 27-31

5. Seaward (1994). *SEAPILE™ Composite Marine Piling Technical Manual,* Seaward International, Inc. PO Box 98, Clearbrook, VA 22624.

6. ASTM D 695 Standard Test Method for Compressive Properties of Rigid Plastics, ASTM vol. 8.01.

7. Langharr, H. (1951) *Dimensional Analysis and Theory of Models*, Wiley, New York

8. Huntly H. (1952) *Dimensional Analysis*, McDonald & Co. Ltd., London

9. Iskander, M and Hassan, M. (2001) "Accelerated Degradation of Recycled Plastic Piling in Aggressive Soils," ASCE Journal of Composites for Construction, August, Vol.5, No. 3

10. Iskander, M Mohamed A. and Hassan, M. (2002) "Durability of Recycled FRP Piling in Aggressive Environments," *in press*, Transportation research Board

LIST OF TABLES & FIGURES

Table 1 — Regression Parameters for Exponential fit of all Specimen Sizes

Strain	m_0 (kN/m^2)	Average m_o	m_1 (1/cm)	Average m_1
10%	3.76		0.15	**0.15**
	3.6		0.14	
	3.4		0.14	
	3.4		0.17	
5%	2.88		0.15	**0.15**
	2.67		0.15	
	2.64		0.15	
	2.8		0.16	
2%	1.3		0.18	**0.175**
	1.02		0.19	
	0.95		0.20	
	1.88		0.13	
1%	0.69		0.20	**0.18**
	0.49		0.19	
	0.32		0.24	
	1.4		0.09	

Fig. 1 — Photograph of Seapile™ (Top) and Wafers Extracted from Seapile™ Core Showing the Location of Punched Specimens (Bottom)

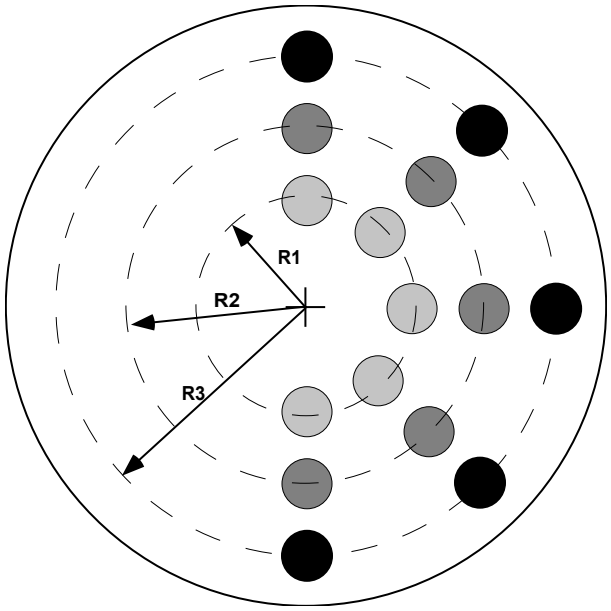

Fig. 2 — Schematic Diagram Showing The Locations Where Specimens were Punched

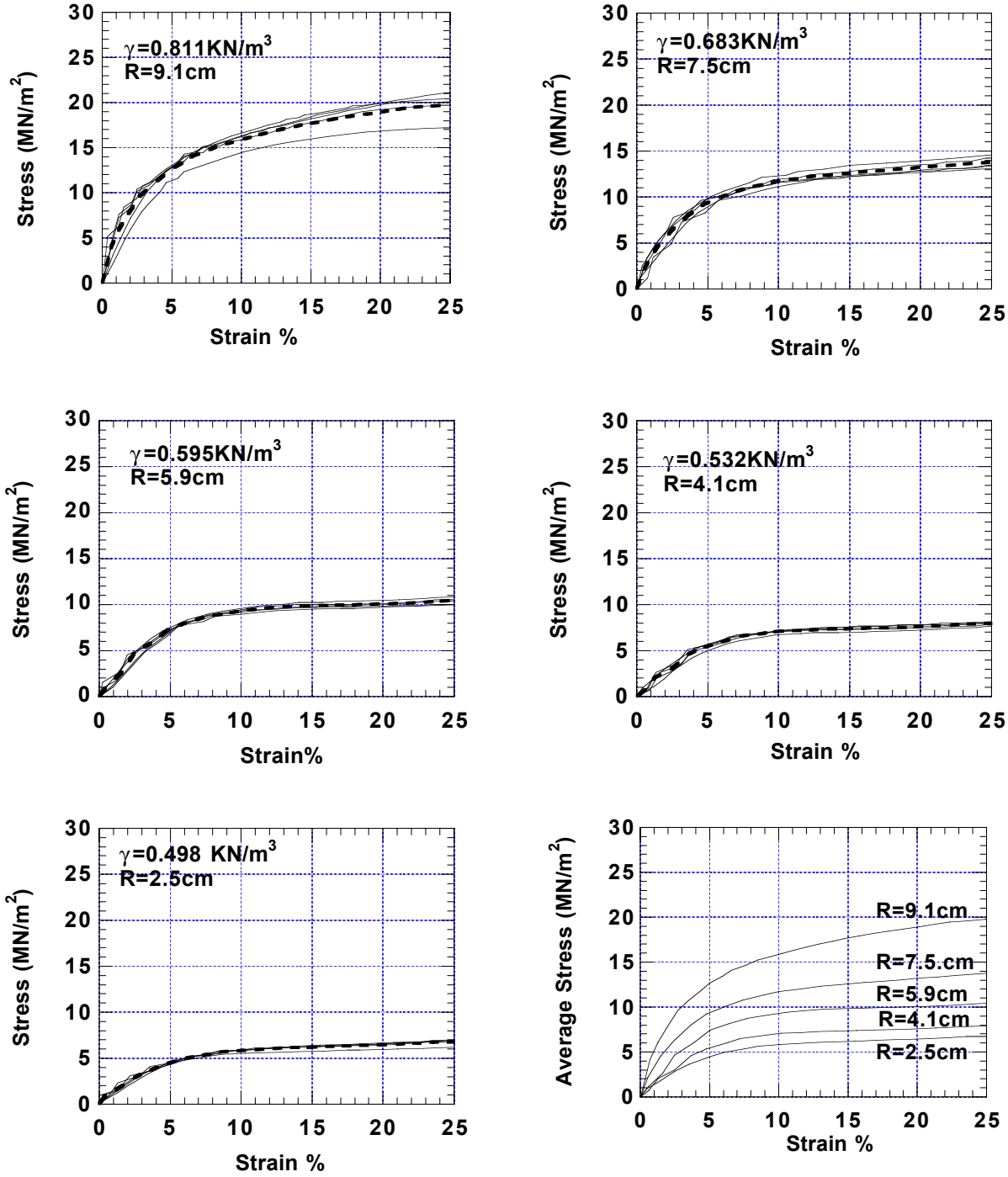

Fig. 3 — Stress Strain Curves for 6.4 mm (1/4 in) Diameter Specimens

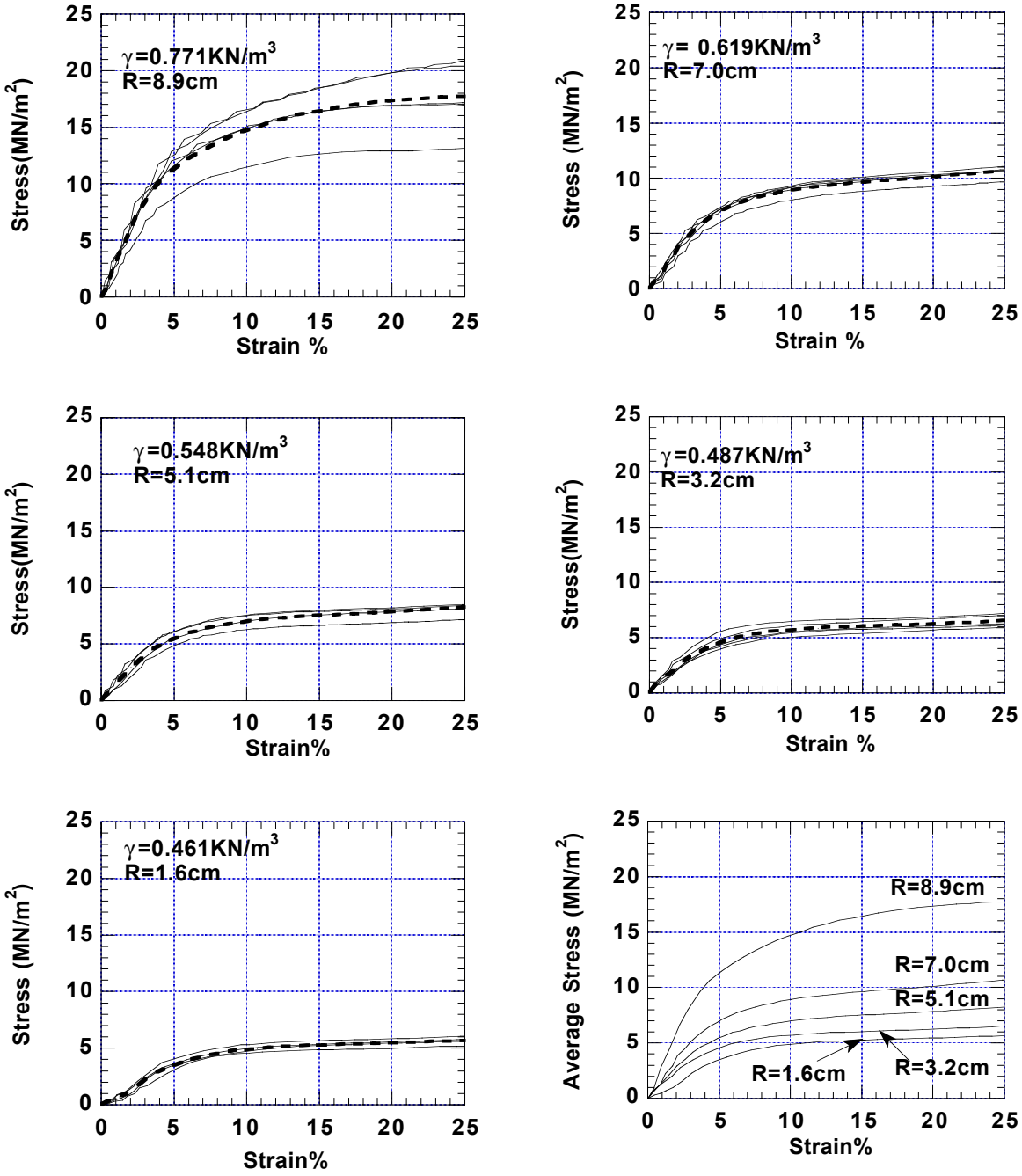

Fig. 4 — Stress Strain Curves for 9.5 mm (3/8 in) Diameter Specimens.

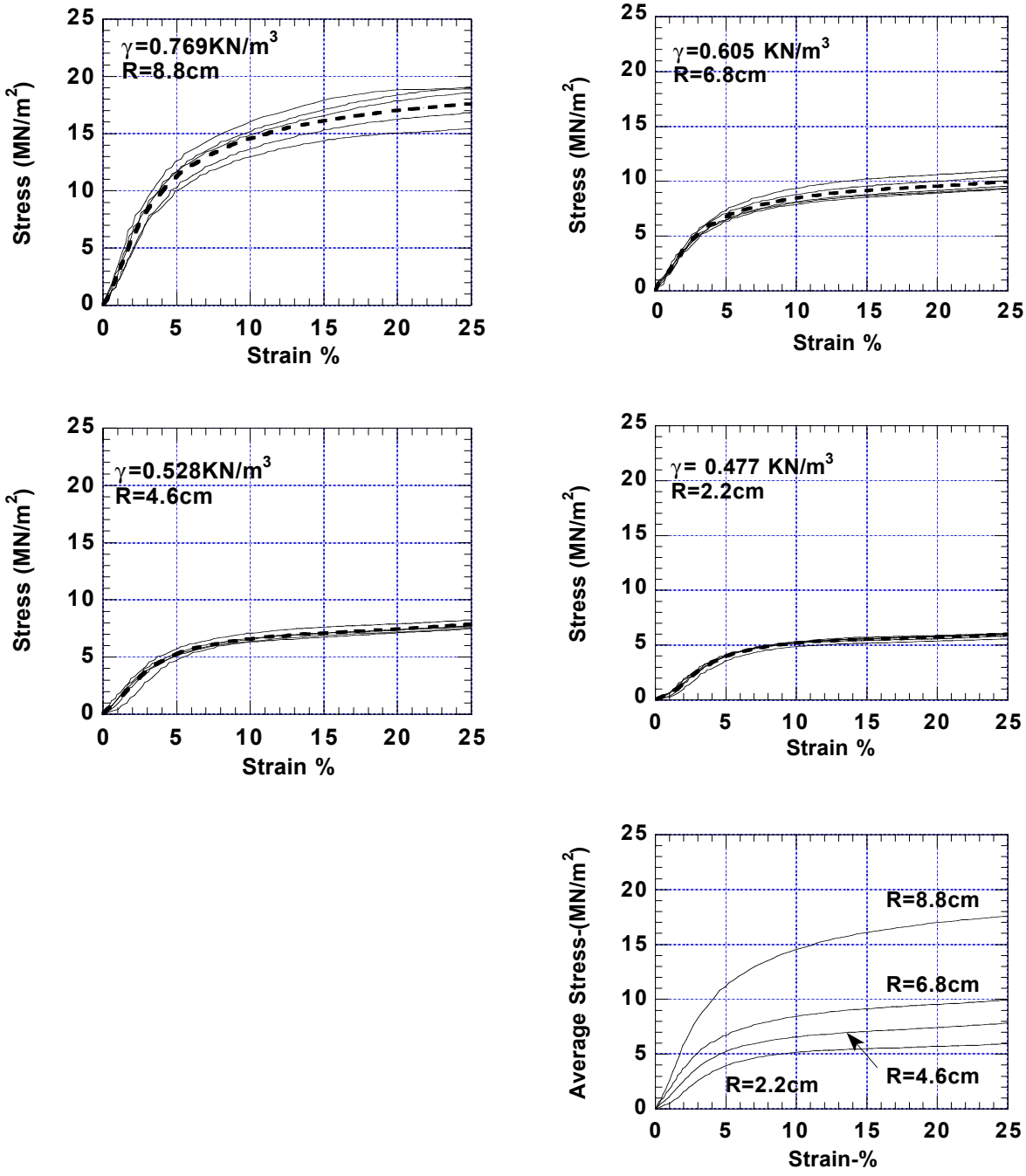

Fig. 5 — Stress Strain Curves for 12.7 mm (1/2 in) Diameter Specimens.

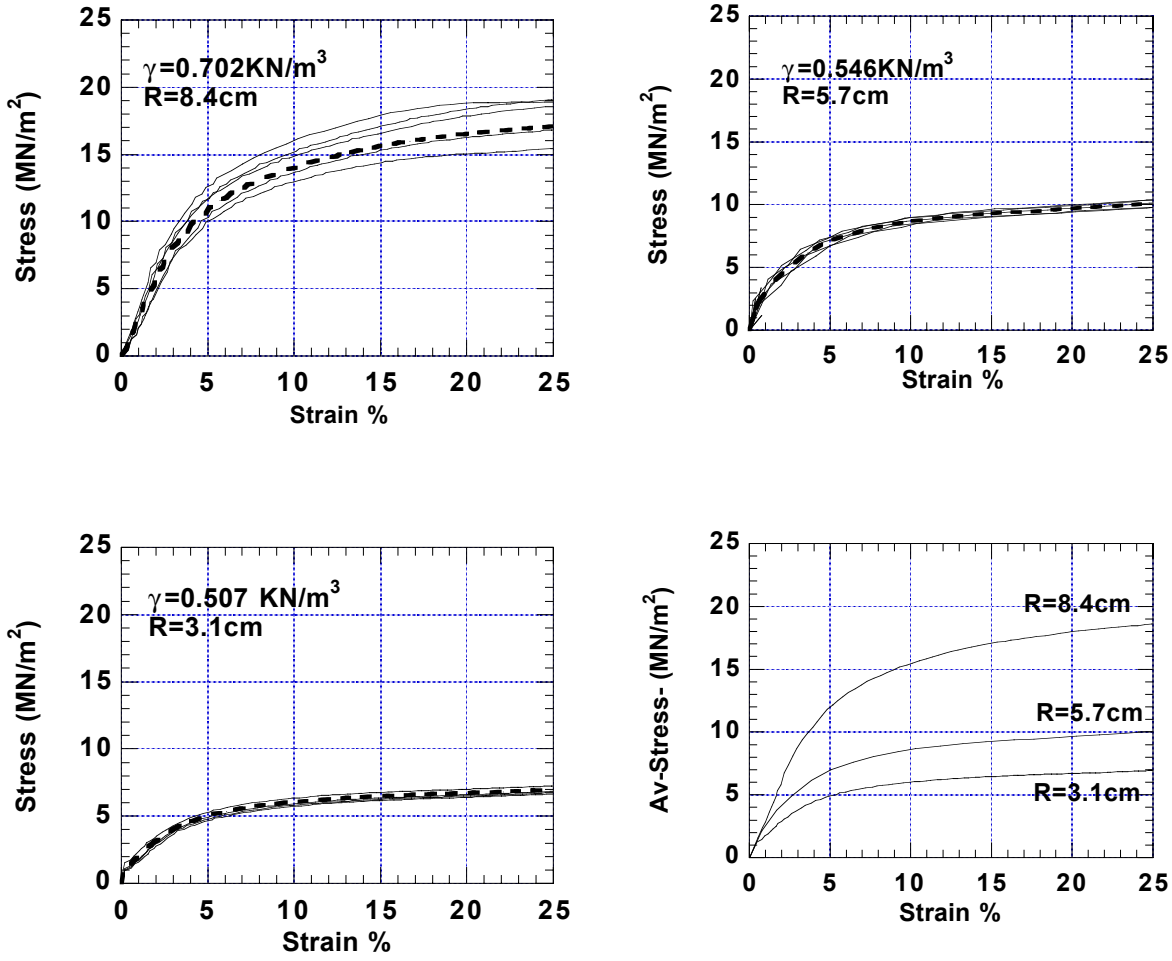

Fig. 6 — Stress Strain Curves for 19.1 mm (3/4 in) Diameter Specimens.

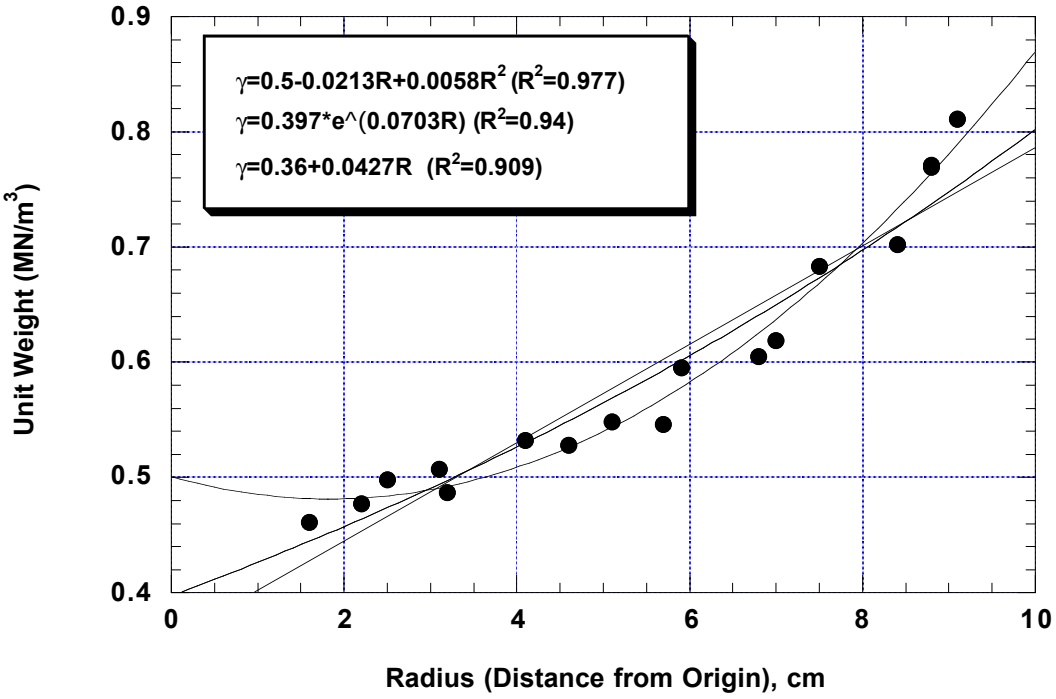

Fig. 7 — Typical Strength Distribution Within the Cross Section (ε = 10%).

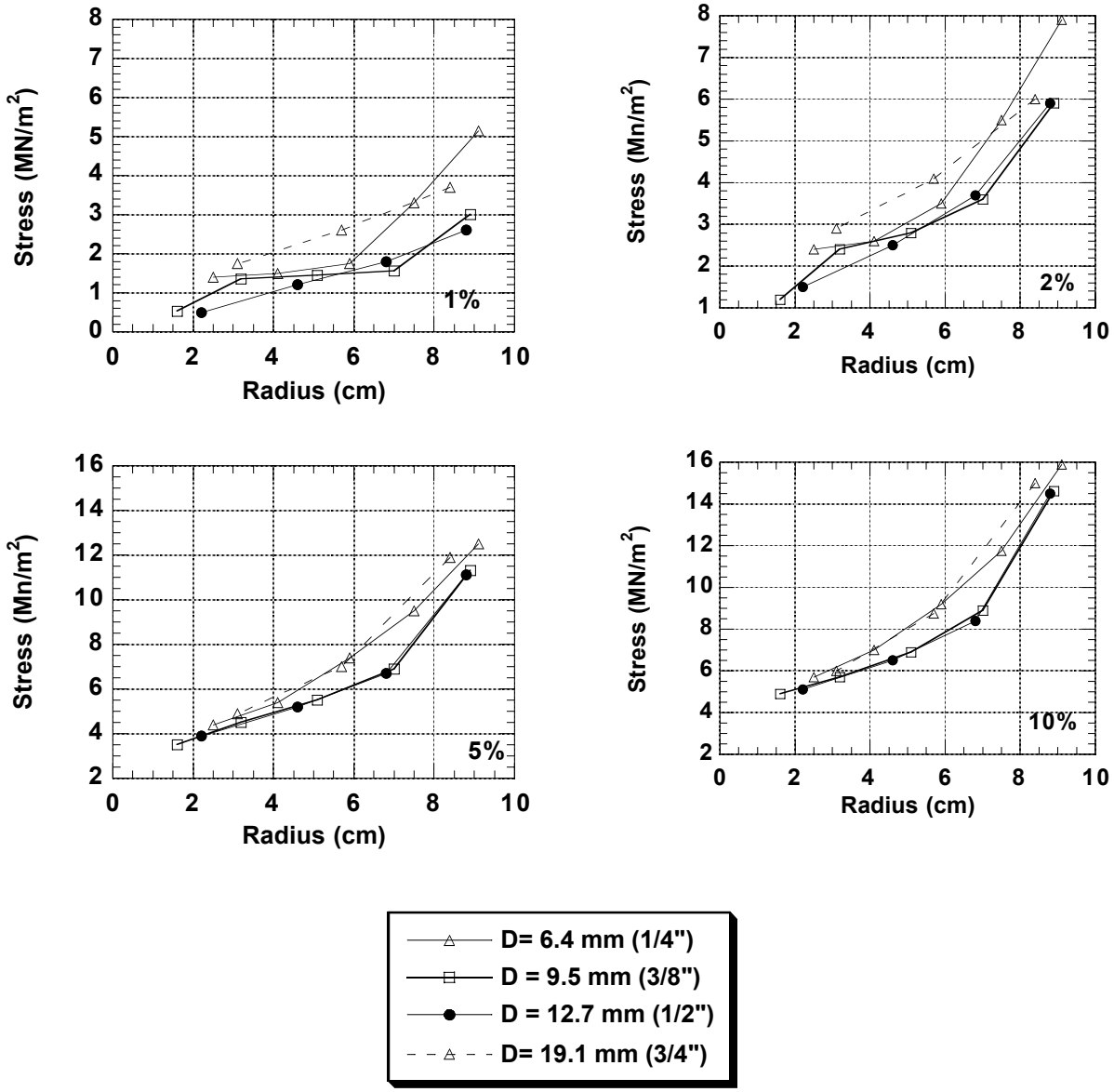

Fig. 8 — Spatial Distribution of Strength at 1%, 2%, 5%, and 10% Strain.

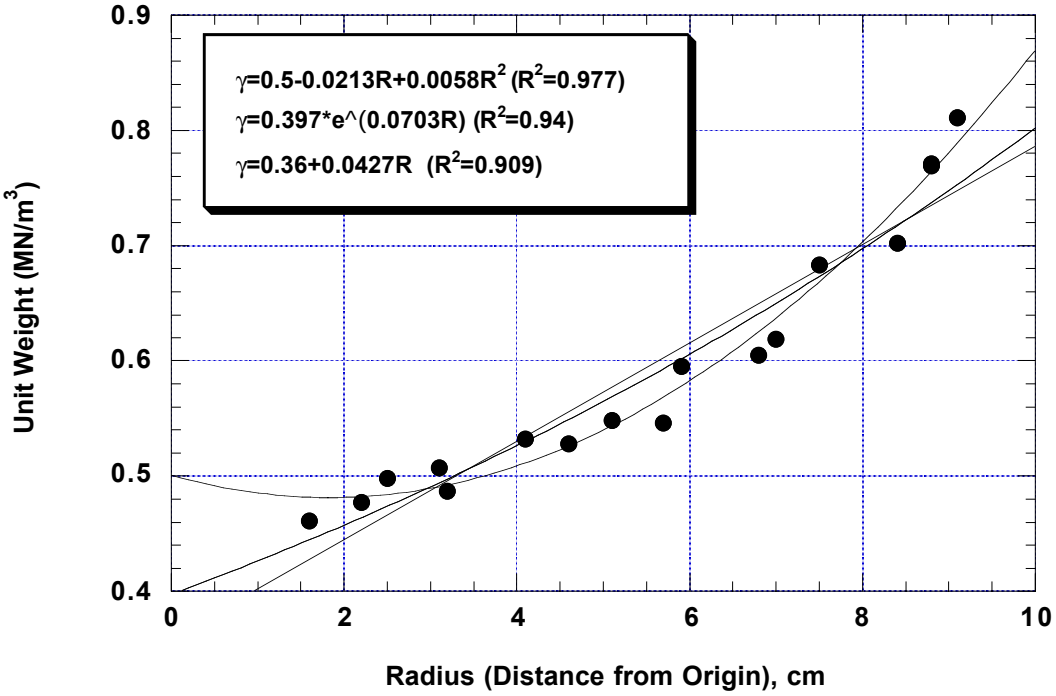

Fig. 9 — Density Distribution Within the Cross Section.

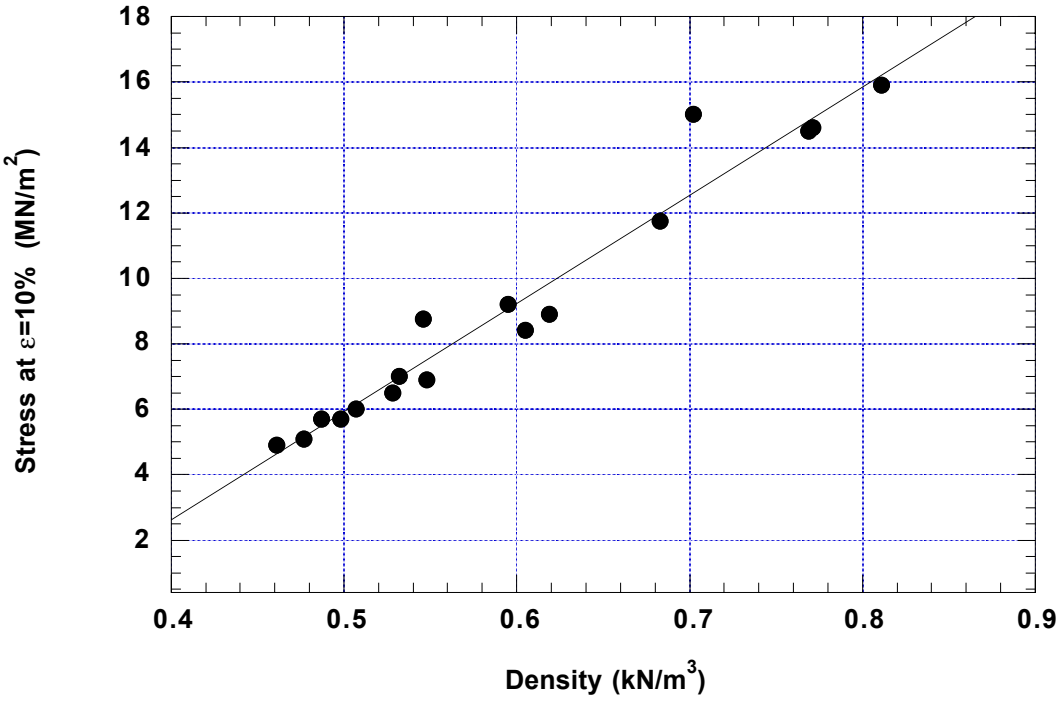

Fig. 10 — Linear Relationship Between Density and Strength Measured at 10% Strain For All Tested Specimens.

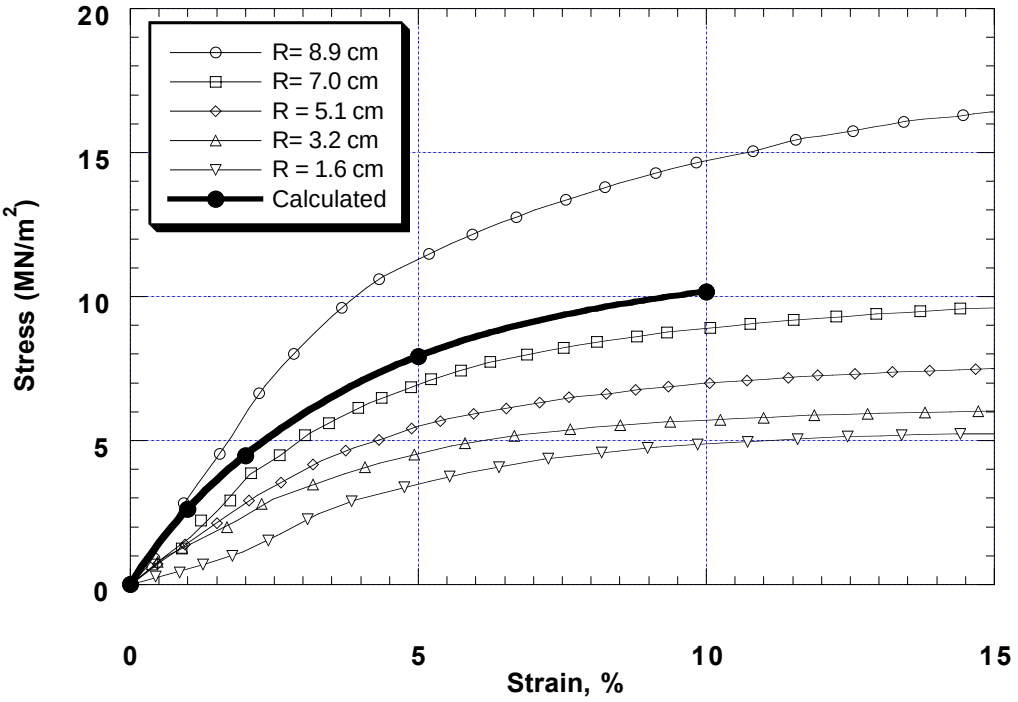

Fig. 11 — Calculated Stress Strain Curve of Full Scale Specimen (Heavy Line) Superimposed on the Average Stress Strain Curves of 9.5-mm (3/8") Diameter Specimens (Thin Lines)

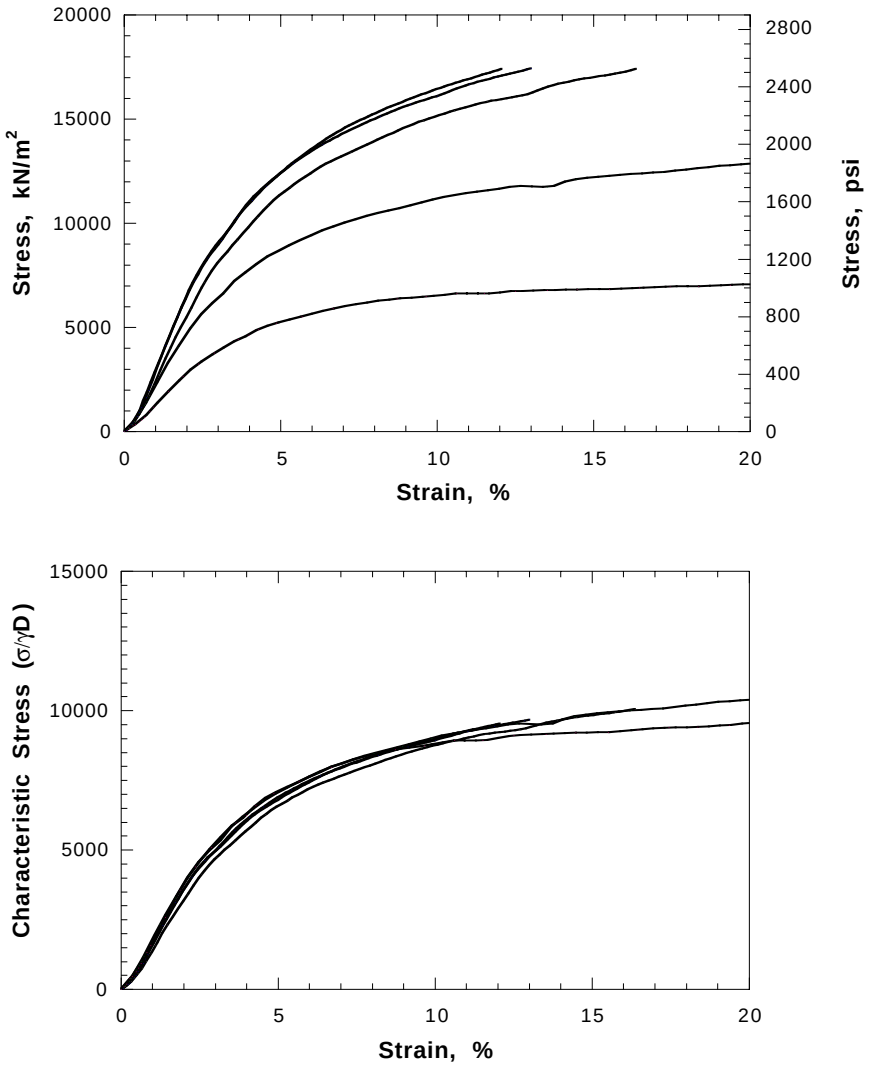

Fig. 12 — (a) Conventional Stress Strain Curves of Specimens Taken From The Same Pile (top). (b) Characteristic Strength vs. Strain Curves for the Curves Shown in (a) (bottom)

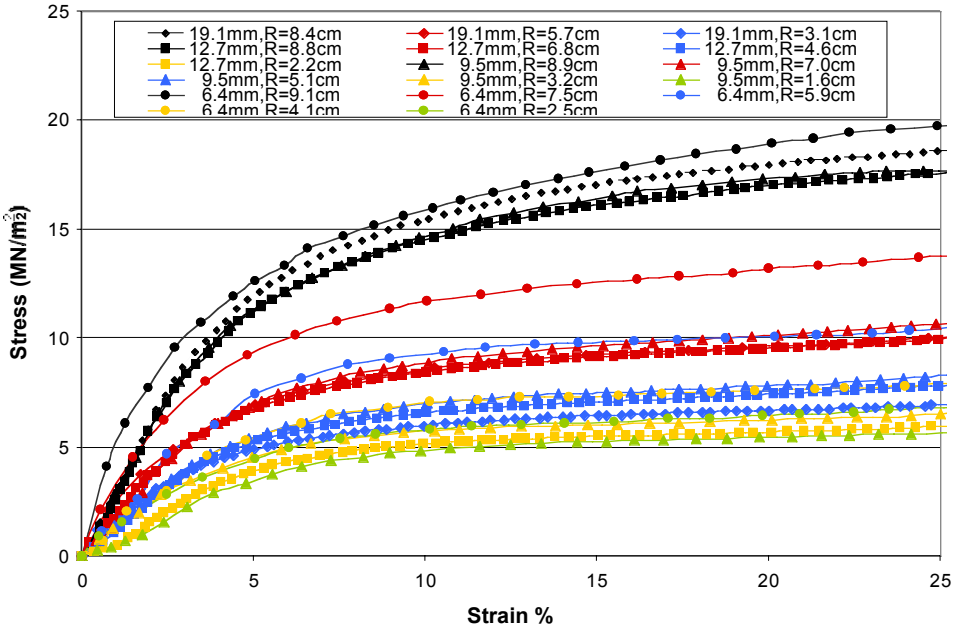

Fig. 13 — Average Stress Strain Curves of all Specimens

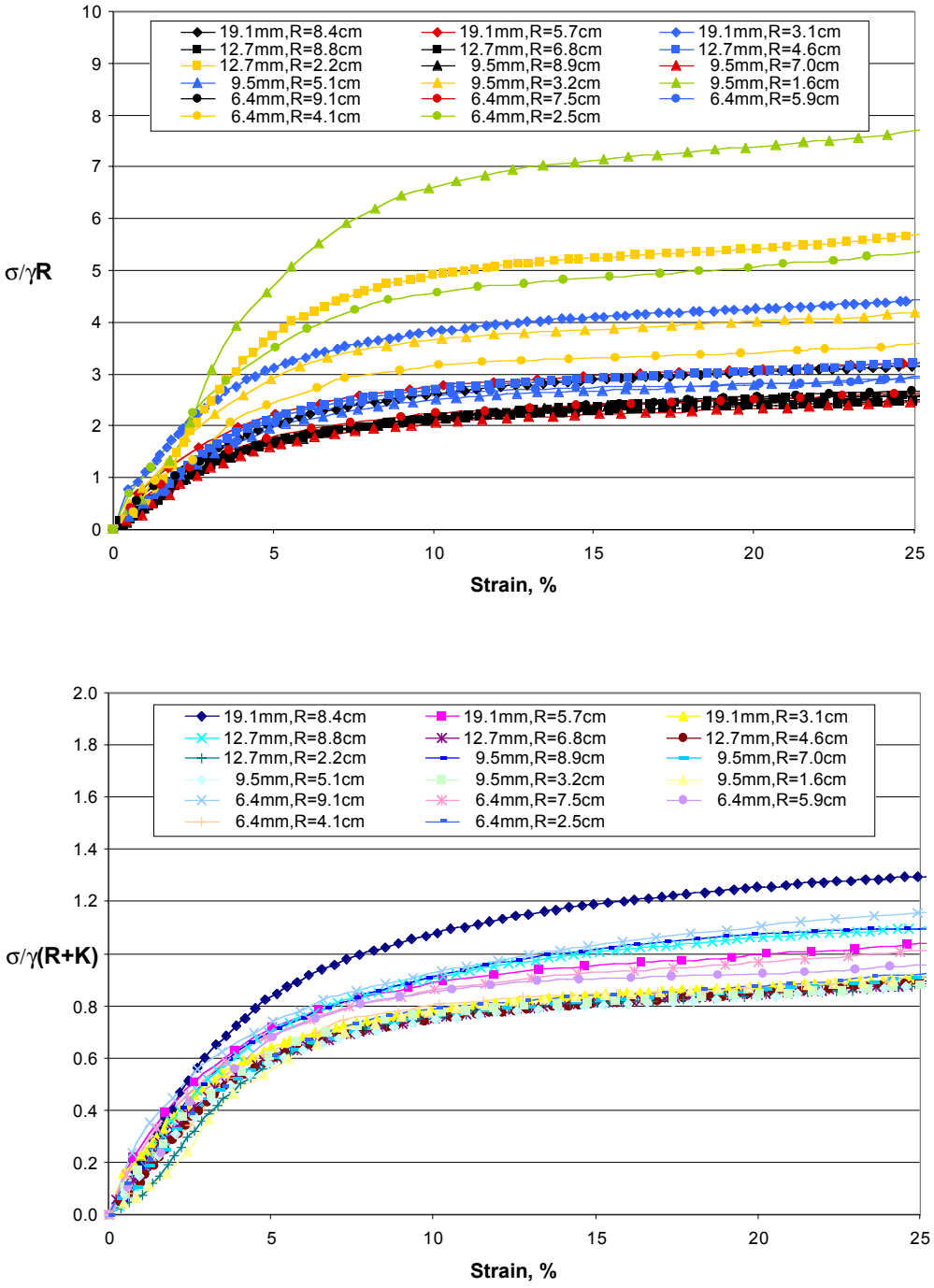

Fig. 14 — Data Normalization of the Conventional Stress Strain Curves Shown in Fig. 13 using Two Methods. (a) Characteristic Stress $\pi=\sigma/\gamma R$ (top), and (b) Modified Characteristic Stress, $\pi_m=\sigma/\gamma(R+K)$